

## RESEARCH LETTER

10.1002/2017GL072956

## Key Points:

- Flickering aurora with a patchy structure varying every 1/160 s was detected by ground-based high-speed imaging observation
- The rapidly varying flickering aurora sporadically appeared on time scales of 0.1 s, with smaller patch structure than typical one
- Flickering auroras are likely to be generated by multi-ion electromagnetic ion cyclotron waves

## Supporting Information:

- Supporting Information S1
- Movie S1
- Movie S2

## Correspondence to:

Y. Fukuda,  
yoko.f@eps.s.u-tokyo.ac.jp

## Citation:

Fukuda, Y., R. Kataoka, H. A. Uchida, Y. Miyoshi, D. Hampton, K. Shiokawa, Y. Ebihara, D. Whiter, N. Iwagami, and K. Seki (2017), First evidence of patchy flickering aurora modulated by multi-ion electromagnetic ion cyclotron waves, *Geophys. Res. Lett.*, **44**, 3963–3970, doi:10.1002/2017GL072956.

Received 6 FEB 2017

Accepted 23 APR 2017

Accepted article online 25 APR 2017

Published online 13 MAY 2017

## First evidence of patchy flickering aurora modulated by multi-ion electromagnetic ion cyclotron waves

Yoko Fukuda<sup>1,2</sup>, Ryuho Kataoka<sup>2,3</sup>, Herbert Akihito Uchida<sup>3</sup>, Yoshizumi Miyoshi<sup>4</sup>, Donald Hampton<sup>5</sup>, Kazuo Shiokawa<sup>4</sup>, Yusuke Ebihara<sup>6</sup>, Daniel Whiter<sup>7</sup>, Naomoto Iwagami<sup>1</sup>, and Kanako Seki<sup>1</sup>

<sup>1</sup>Department of Earth and Planetary Science, University of Tokyo, Tokyo, Japan, <sup>2</sup>National Institute of Polar Research, Tokyo, Japan, <sup>3</sup>Department of Polar Science, The Graduate University for Advanced Studies (SOKENDAI), Tokyo, Japan, <sup>4</sup>Institute for Space-Earth Environmental Research, Nagoya University, Nagoya, Japan, <sup>5</sup>Geophysical Institute, University of Alaska Fairbanks, Fairbanks, Alaska, USA, <sup>6</sup>Research Institute for Sustainable Humanosphere, Kyoto University, Kyoto, Japan, <sup>7</sup>School of Physics and Astronomy, University of Southampton, Southampton, UK

**Abstract** Electromagnetic ion cyclotron (EMIC) waves, one of the possible origins of flickering aurora, have been thought to modulate the electron flux at a few thousand kilometers. In fact, flickering aurora with a frequency range of 3–15 Hz has often been identified by ground-based optical observations and has been interpreted to be caused by O<sup>+</sup>-band EMIC waves. However, extant research to date has not identified possible signatures of H<sup>+</sup>-band EMIC waves due to technical limitations of ground-based high-speed imagers. The present study shows the first evidence that patchy flickering aurora could be modulated by H<sup>+</sup>-band EMIC waves, based on the data obtained from imaging observations at 160 frames per second. The sporadic appearance of the flickering aurora in the frequency range of 50–80 Hz coexisted with typical flickering auroras of approximately 10 Hz. These results are consistent with the hypothesis that flickering auroras are generated by multi-ion EMIC waves.

## 1. Introduction

Flickering aurora is characterized by periodic luminosity oscillations and typically appears within active and bright auroral arcs immediately prior to and during auroral breakup [Beach et al., 1968; Berkey et al., 1980; Kunitake and Oguti, 1984; Sakanoi and Fukunishi, 2004]. The typical frequency range is 3–15 Hz [e.g., Paulson and Shepherd, 1966; Beach et al., 1968], which is comparable to the oxygen ion cyclotron frequency at altitudes of a few thousand kilometers in which the acceleration region and the cavity region are located. In order to explain the generation mechanism of flickering aurora, Temerin et al. [1986] proposed the Landau resonance interaction between electrons and electromagnetic ion cyclotron (EMIC) waves as a cause of electron flux modulations. Sakanoi et al. [2005] and Gustafsson et al. [2008] reported that spatiotemporal variations of flickering patches can be interpreted by the interference wave patterns of EMIC waves. Due to the aforementioned reasons, flickering aurora observed to date is not inconsistent with EMIC waves.

In a multi-ion species plasma, H<sup>+</sup>-band EMIC waves with frequencies between the cyclotron frequency of helium ions,  $f_{\text{He}^+}$ , and that of protons,  $f_{\text{H}^+}$ , were identified by in situ satellite observations [e.g., Gurnett and Frank, 1972; Temerin and Lysak, 1984; Gustafsson et al., 1990; Erlandson and Zanetti, 1998]. McFadden et al. [1998] reported the simultaneous observation of H<sup>+</sup>-band EMIC waves and the flux modulation of field-aligned electrons with the same frequency as the wave by using the FAST satellite, which was predicted based on a simulation study by Temerin et al. [1993]. As reported by previous studies, the propagation properties of EMIC waves in a multi-ion plasma are more complicated than those in a single species [Smith and Brice, 1964]. Gustafsson et al. [1990] also reported that He<sup>+</sup>-band events at frequencies between the cyclotron frequency of oxygen ions,  $f_{\text{O}^+}$ , and that of  $f_{\text{He}^+}$  were observed by the Viking satellite, although it was revealed by ray tracing calculations that these waves are typically difficult to detect because He<sup>+</sup>-band waves tend to latitudinally spread out when compared with H<sup>+</sup>-band and O<sup>+</sup>-band waves with frequencies  $< f_{\text{O}^+}$  [Lund and LaBelle, 1997]. These satellite observations imply the possibility that both He<sup>+</sup>-band and H<sup>+</sup>-band EMIC waves contribute to produce high-frequency flickering auroras.

McHarg et al. [1998] found broadband auroral intensity fluctuations in the range of 35–60 Hz and with a maximum frequency of 180 Hz by using a ground-based high-speed photometer, and these fluctuations were

interpreted as lighter ions such as  $\text{He}^+$  or  $\text{H}^+$ . Recently, *Yaegashi et al.* [2011] determined that approximately one third of flickering events involved broadband frequencies in the range of 20–50 Hz by using high-speed imaging. The flickering events were interpreted as caused by  $\text{He}^+$ -band EMIC waves as opposed to  $\text{O}^+$ -band EMIC waves. However, the time resolution of the imaging system was not sufficiently high to detect variations  $>50$  Hz due to the 100 frames per second (fps) sampling.

The purpose of this study is to test the hypothesis that flickering auroras are generated by multi-ion EMIC waves by realizing a ground-based high-speed imaging observation with a sampling rate of 160 fps. The instrumentation used in the study is described in section 2. Section 3 provides an event description of the fastest flickering aurora and the results of the spatiotemporal analyses. The possibility of  $\text{H}^+$ -band EMIC waves as a source of the fastest ever observed flickering modulation is discussed in section 4. The conclusions are summarized in section 5.

## 2. Instrumentation

Two scientific complementary metal-oxide semiconductor (sCMOS) cameras (ORCA-Flash 4.0V2, Hamamatsu Photonics, Hamamatsu, Japan) were installed at Poker Flat Research Range (PFRR, 65.74° MLAT,  $L = 5.9$ ) in Alaska from January to April in 2016. The two cameras, hereafter referred to as CMOS 1 and CMOS 2, were directed to the magnetic zenith at PFRR. In order to increase the signal-to-noise ratio and the sampling rate, the original  $2048 \times 2048$  pixel images were reduced to  $512 \times 512$  pixel images by  $4 \times 4$  binning. CMOS 1 was equipped with a narrow field-of-view (FOV) lens (NIKKOR 50 mm F1.2) to investigate the fine-scale high-speed morphology, and only partial images of  $512 \times 256$  pixels across the magnetic zenith were recorded at 160 fps. The 160 fps sampling rate was designed to cover typical cyclotron frequencies of three ion components ( $\text{O}^+$ ,  $\text{He}^+$ , and  $\text{H}^+$ ), which typically correspond to 10 Hz, 40 Hz, and 160 Hz, respectively. The FOV of CMOS 1 was approximately  $14.8^\circ \times 7.4^\circ$  and corresponded to an area of  $26 \text{ km} \times 13 \text{ km}$  at a height of 100 km. CMOS 2, equipped with a wide FOV lens (NIKKOR Fisheye 8 mm F2.8), was used to monitor the mesoscale auroral morphology, and  $512 \times 512$  pixel images were recorded at 40 fps. The FOV of CMOS 2 corresponded to  $100^\circ \times 100^\circ$ .

The stability of the acquisition frame rate was improved in the winter of 2016 when compared with that of the former sCMOS camera systems presented in studies by *Kataoka et al.* [2015] and *Fukuda et al.* [2016]. A new circuit board was designed to generate 160 fps trigger signals and release the shutter of the camera based on the Global Navigation Satellite Systems (GNSS) time information. Each camera system possessed its own circuit board with a microprocessing unit (MPU) that was used to communicate with the PC, trigger the shutter signal, and control the LEA-M8F (u-blox) GNSS module. The GNSS module provided time information with a time pulse accuracy  $\leq 20$  ns and a frequency accuracy  $< 5$  ppb to synchronize the MPU.

## 3. Observational Results

### 3.1. Event Description

Flickering aurora was observed in the premidnight sector ( $\sim 21.5$  magnetic local time) during the auroral breakup at the expansion phase of a substorm with a peak AE index of 1266 nT at 0906 UT on 19 March 2016. Ground-based magnetometer data recorded at PFRR are shown in Figure 1a. H, D, and Z indicate the north-south, east-west, and vertical geomagnetic field components, respectively. Figure 1b shows the approximate magnetic north-south keogram for 20 min that is created from the data obtained from CMOS 2. The location of the magnetic zenith at PFRR is marked by a white horizontal dashed line. An intensity time profile at the magnetic zenith is shown in Figure 1c. Flickering auroras were detected at the particular time when the extremely bright aurora exceeding a few hundred kR at 557.7 nm (not shown) appeared around the magnetic zenith, which is denoted by a white vertical dashed line in Figure 1b. Flickering auroras were observed within active auroras for a time period of approximately 1 min from 09:05:55 UT by CMOS 1. The active auroras including flickering auroras appeared simultaneously with a large change in the horizontal component of the geomagnetic field of approximately 300 nT as shown by a black vertical line in Figure 1a.

The active aurora consisting of the fine-scale turbulent motions was detected by CMOS 1. The flickering aurora was observed at 09:06:26–09:06:29 UT, and the complicated auroral motions began at 09:06:35 UT. Bright arc elements with rapid movements were observed at 09:06:38 and 09:06:40 UT, and flickering auroras

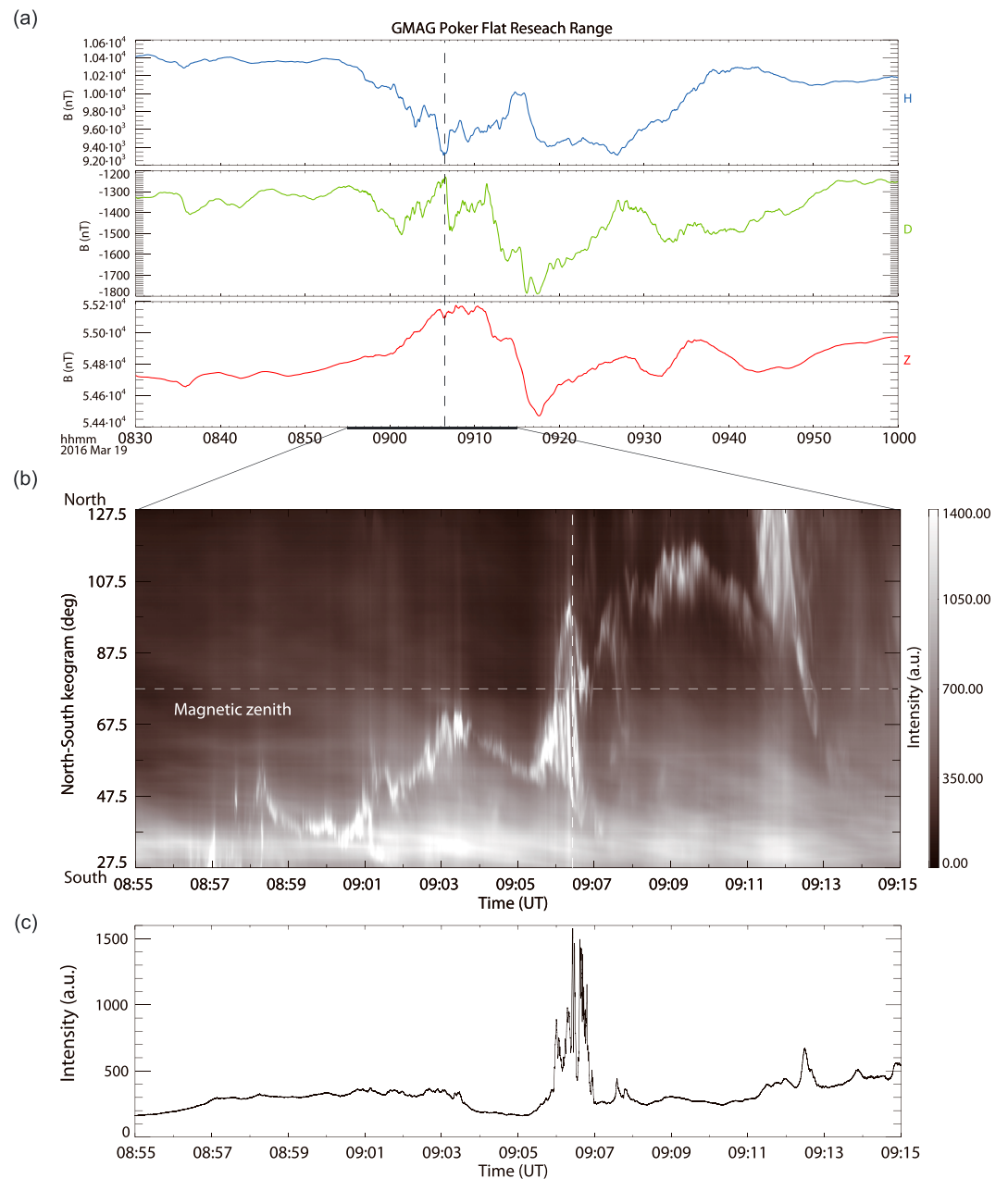


**Figure 1.** (a) Ground-based magnetometer data at PFRR. North-south, east-west, and vertical components are shown as H, D, and Z, respectively. (b) North-south keogram for 20 min created from the data obtained from CMOS 2. (c) Time variation of the auroral intensity around the magnetic zenith shown by a white horizontal dashed line in Figure 1b.

sporadically appeared again from 09:06:38 UT. The time sequence of the aforementioned active auroras for 1 min is shown in Movie S1 in the supporting information. A few “arc packets,” which were similar to what was previously reported in a study by Semeter *et al.* [2008], were detected at time intervals of 09:06:35.5 UT and 09:06:43.0 UT.

### 3.2. Spatiotemporal Analyses

The fastest flickering aurora discussed in this study sporadically appeared inside the eastward (leftward in Movie S1) drifting arc system for only 1 s at around 09:06:26.600 UT. Figure 2a shows a snapshot of the flickering aurora observed at 09:06:26.612 UT. A white cross marks the magnetic zenith at PFRR, and a black X and a black diamond denote the selected locations of the fastest flickering aurora and the flickering aurora with a

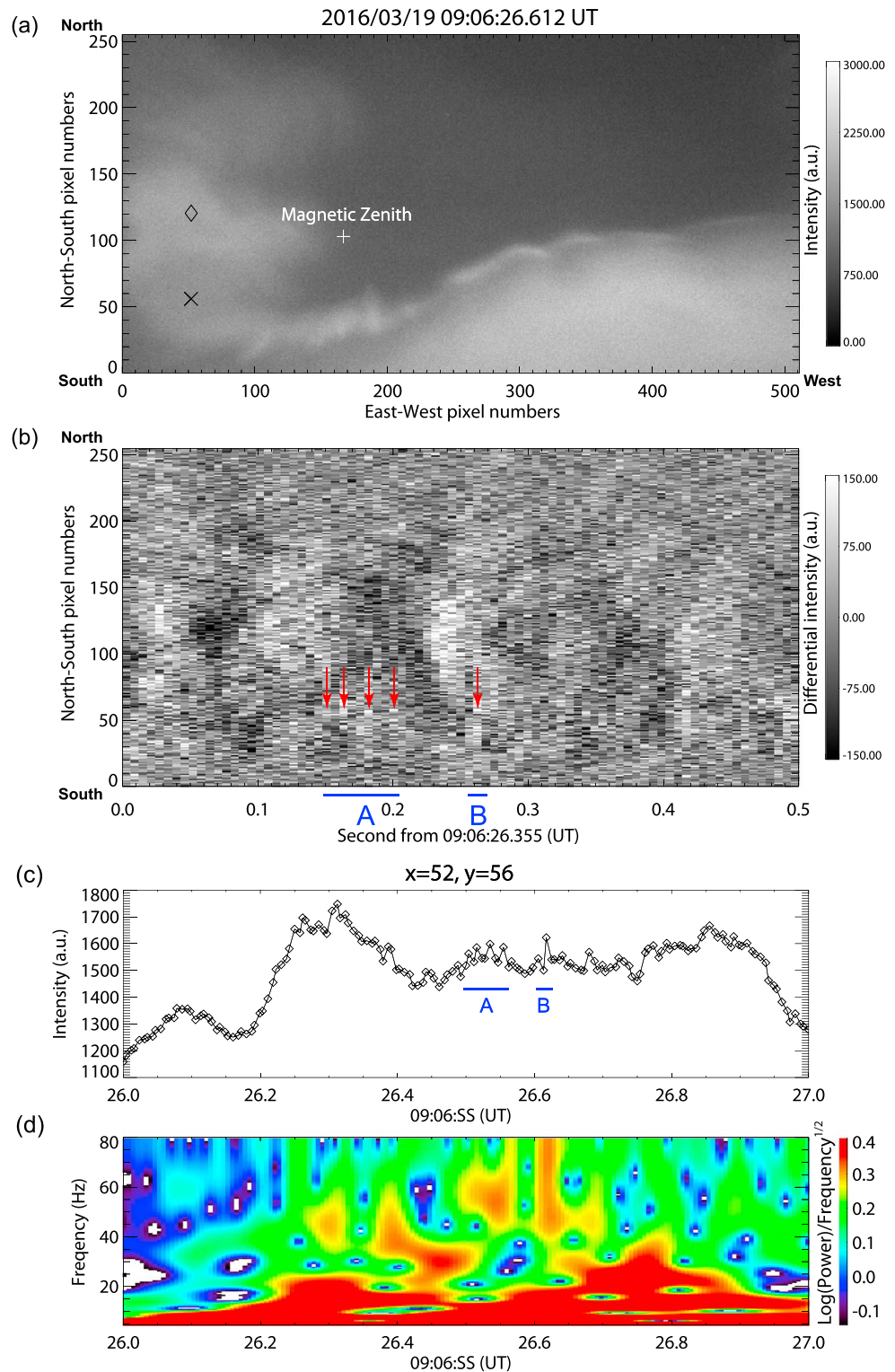


**Figure 2.** (a) Snapshot captured by CMOS 1 when the fastest flickering aurora appeared around a black X ( $x = 52, y = 56$ ). A white cross indicates the magnetic zenith at PFRR, and a black diamond ( $x = 52, y = 120$ ) shows the appearance location of the flickering aurora with a typical frequency. North corresponds to the top, and east corresponds to the left. (b) North-south keogram of the high-frequency components exceeding 10 Hz for 0.5 s from 09:06:26.355 UT across the point X and the diamond. (c) Intensity time profile spatially averaged over a  $5 \times 5$  pixel area centered at the point X. (d) Frequency-time representation calculated from the S-transform using the intensity profile for 1 s from 09:06:000 UT. The color shows a logarithm power spectrum normalized by the square root of each frequency.



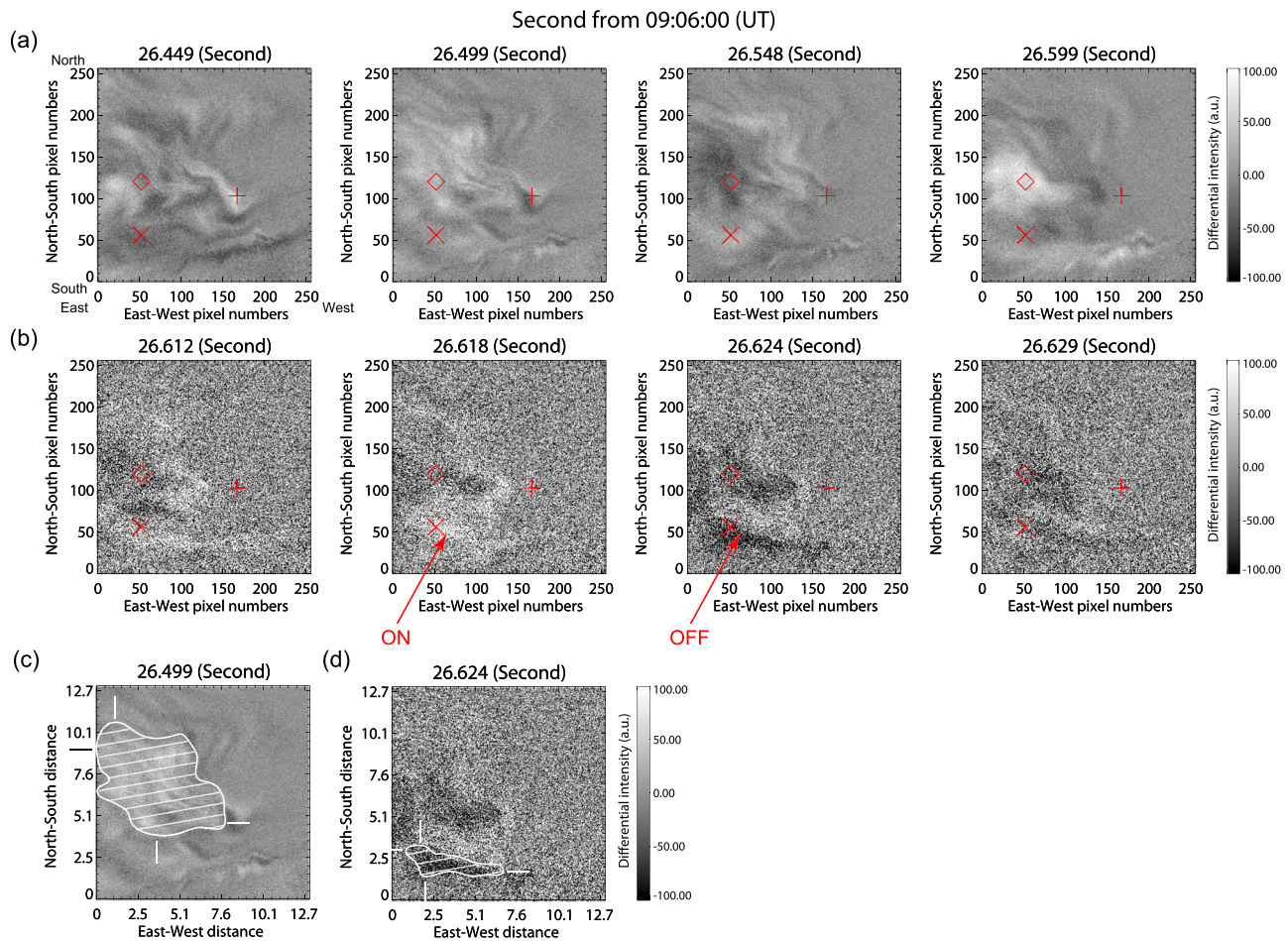


**Figure 3.** Time variations of the flickering patch structures that appear in an extracted  $256 \times 256$  pixel region. (a) Typical 10 Hz flickering aurora represented by the running average of high-pass filtered images during a 0.15 s time interval. (b) Flickering aurora with temporal variation of the patch structure varying every  $1/160$  s represented by subtracting high-pass filtered images from a previous frame during the 0.02 s time interval B. (c) The patch shapes and scales with the frequency equal to 10 Hz, which is shown on the second panel of Figure a, and (d) the fast variations varying every  $1/160$  s, which is shown on the third panel of Figure 3b, at the altitude of 100 km, respectively.

typical frequency, respectively. We consider that the temporal variation is dominant as shown in Figure 3 (discussed later), and the flickering frequency was estimated using the S-transform method [Stockwell *et al.*, 1996]. In order to determine the location of the fastest flickering aurora accurately, the 2-D maps of the power spectrum from 1 to 80 Hz for each frame were calculated from the S-transform, and the point X was selected from pixels in which the power spectral density at 75 Hz at 09:06:12 UT was the highest (not shown). Figure 2b shows the approximate magnetic north-south keogram of the data obtained from CMOS 1 with higher frequency components exceeding 10 Hz (hereafter referred to as high-pass filtered images) across point X and the diamond for 0.5 s from 09:06:26.355 UT, which is created from the subtraction of running averaged images with a 0.1 s time window at each frame. The time intervals labeled as A and B indicate the time periods of flickering auroras focused on in this study. Flickering aurora with a frequency of approximately 10 Hz was observed around the  $x = 70$ – $150$  pixel region. The 1 s time variation in the flickering aurora from 09:06:26.000 UT is shown in Movie S2, which involves a slow-motion movie played at a quarter of the real speed.

Figure 2c depicts the intensity time profile averaged over a  $5 \times 5$  pixel area centered at point X as shown in Figure 2a. Figure 2d shows the frequency-time representation corresponding to 5–80 Hz, which is calculated from the S-transform using the intensity profile to investigate the short time scale variation of the flickering frequency. The color indicates the logarithmic power spectrum normalized by the square root of each frequency. The results indicate that sporadic intensifications of spectral power over 20 Hz were observed for

0.4 s from 09:06:26.3 UT around the point X. Four bipolar waveforms and a waveform that was especially observed during time intervals A and B covered frequency ranges of approximately 50–60 Hz and to a maximum corresponding to the Nyquist frequency of 80 Hz, respectively. Each flickering amplitude was approximately 1.6% and 3.2% of the background aurora and was significant,  $>3\sigma$  and  $>6\sigma$ , respectively, where  $\sigma$  is a noise level corresponding to  $\sim 14$  counts. The amplitude ratios were 6–7 times lower than the typical flickering aurora, which is reported as 10%–20% of the background aurora [e.g., Berkey *et al.*, 1980; Kunitake and Oguti, 1984; Sakanoi and Fukunishi, 2004; Whiter *et al.*, 2010].

Figure 3 shows the time variation of flickering patch structures that appear within an extracted  $256 \times 256$  pixel region. The running average of the high-pass filtered images with a 0.05 s time window was calculated to investigate the patch scale of the typical 10 Hz flickering aurora. Figure 3a shows the running average images of a 0.05 s time interval for 0.15 s from 09:06:26.449 UT. It was observed that the flickering patch is roughly circular in shape with an approximately  $100 \times 100$  pixel scale. Figure 3c represents the patch shape at 09:06:26.499 UT, which corresponds to the second panel of Figure 3a, and the patch scale is estimated to be  $7.0 \text{ km} \times 7.8 \text{ km}$  in the approximate magnetic north-south and east-west directions based on a white contour under the assumption that the emission layer of the flickering aurora is at an altitude of 100 km. Figure 3b shows the time variation in differential images that are created by subtracting the high-pass filtered image from a previous frame during time interval B corresponding to 0.02 s. It is found that a clear on-off modulation varying every  $1/160$  s appeared at  $\sim 5$  km equatorward from the center of the typical flickering aurora. Figure 3d represents the patchy structure at 09:06:26.624 UT, which corresponds to the third panel of Figure 3b. The patch shape is highly aligned in the east-west direction, and the scale is approximately  $1.9 \text{ km} \times 5.9 \text{ km}$  in the north-south and east-west directions. It is also found that the patch scale of the fastest flickering aurora is smaller than that of the typical flickering aurora.

#### 4. Discussion

In this study, we obtained 2-D images of the fastest ever observed flickering aurora with the temporal variation of the patchy structure varying every  $1/160$  s. The flickering aurora with frequencies  $>20$  Hz sporadically appeared within the bright breakup arc of more than a few hundred kR, and the peak frequency intermittently changed on a time scale of 0.1 s during a 0.4 s period from 09:06:26.3 UT. The durations of the time intervals A and B corresponded to 0.05 s and  $<0.02$  s, respectively. The fast flickering aurora was located equatorward of the typical flickering aurora with a frequency of 10 Hz, and the spatial distance between the centers of each patch approximately corresponded to 5 km at an altitude of 100 km. The patch was aligned in the east-west direction on the spatial scale of  $1.9 \text{ km} \times 5.9 \text{ km}$ , which was smaller than those of the roughly circular 10 Hz flickering aurora on the scale of  $7.0 \text{ km} \times 7.8 \text{ km}$  in the north-south and east-west directions. McHarg *et al.* [1998] used a high-speed 1-D photometer to acquire temporal variations of aurora up to 20 kHz. They found that intensity fluctuations were primarily below 80 Hz, and frequencies up to 180 Hz were also detected. As far as we know, the 2-D structure of such a fast-varying flickering aurora has not been reported until now.

The origin of the fastest flickering aurora with the temporal variation of the patchy structure varying every  $1/160$  s can be interpreted as  $\text{H}^+$ -band EMIC waves due to the following reasons. The observational results show that the typical flickering frequency was approximately 10 Hz. Consequently, the resonance altitude between electrons and  $\text{O}^+$ -EMIC waves can be estimated as 6000 km. Multi-ion EMIC waves in  $\text{O}^+$ ,  $\text{He}^+$ , and  $\text{H}^+$  generally have the frequency depending on the propagation angle. Given the assumption that all multi-ion EMIC waves resonate electrons at the same altitude of 6000 km, the frequency range of  $\text{H}^+$ -band EMIC waves with the propagation angle of  $0^\circ$ – $90^\circ$  is 40–160 Hz. It is found that the frequency of the observed fastest flickering aurora possibly corresponds to the lower frequency range of  $\text{H}^+$ -band EMIC waves.

A technical reason for the first-time detection of possible  $\text{H}^+$ -band flickering aurora is that the high-speed imaging observation enabled the detection of the sporadic appearance of the fast flickering aurora on a time scale of 0.1 s with a limited horizontal scale of  $1.9 \text{ km} \times 5.9 \text{ km}$ . Single-point in situ observations by satellites and sounding rockets so far cannot resolve such fast and fine-scale variations.

We now discuss the formation mechanisms for the spatiotemporal behavior of the fastest flickering aurora. The fine-scale flickering structure with a frequency of 80 Hz was east-west aligned and is consistent with

the spatial asymmetric property demonstrated in a study by *Michell et al.* [2012]. A possible reason for the result is the interference pattern composed of multiple EMIC waves with different wave numbers. In addition, the rapidly varying patchy structure appeared at  $\sim 5$  km equatorward from the center of the typical flickering aurora. The spatial gap between these appearances is likely to be associated with the propagation property of multi-ion EMIC waves, which was reported by *Lund and LaBelle* [1997] using ray tracing calculations. They showed that  $H^+$ -band EMIC waves spread over wider latitude range than the  $O^+$ -band EMIC waves and consequently have a lower power spectral density. Although our result showed that the  $H^+$ -band flickering aurora has smaller scale structure than that of typical flickering auroras, further investigations of the spatial distribution and the patch scale of flickering auroras generated by multi-ion EMIC waves are important to clarify the wave property in a multi-ion species plasma.

The temporal variation of the fastest flickering aurora was actually complicated by a sporadic appearance on a time scale of 0.1 s. This feature is likely to be caused by the rapid appearance and disappearance of the multi-ion EMIC waves and indicates that the generation mechanisms are beyond the linear theory due to nonlinear effects as discussed in the inner magnetosphere [*Omura et al.*, 2010]. Although another possibility is a temporal variation of the acceleration region associated with the wave excitation, it is not likely to be reasonable, because the parallel potential drops appear to be stable on time scales corresponding to tens of seconds [*Ergun et al.*, 1998].

Our study could not explain the excitation mechanism of the sporadic multi-ion EMIC waves based solely on the high-speed imaging observations. In order to improve our understanding of the formation mechanisms discussed above, simulation studies of the generation and propagation properties of multi-ion EMIC waves are needed. It is important to consider nonlinear and inhomogeneous effects in order to reproduce observations of complicated spatiotemporal variations.

## 5. Conclusions

We obtained 2-D images of the fastest ever observed patchy flickering aurora varying every 1/160 s from ground-based high-speed observations. The flickering aurora with frequencies  $>20$  Hz sporadically appeared within the bright breakup arc, and the peak frequency intermittently changed on a time scale of 0.1 s during a 0.4 s period. The fast-varying patch was aligned in the east-west direction and was smaller than the roughly circular 10 Hz flickering auroral patch. These results are consistent with the hypothesis that flickering auroras are generated by multi-ion EMIC waves in the inhomogeneous plasma.

## Acknowledgments

We would like to thank Hanna Dahlgren for the constructive discussion and useful comments during Yoko Fukuda's visit to University of Southampton. This work was supported by Grants-in-Aid for Scientific Research (19403010; 25302006; 15H05747; 15H05815; 16H06286) from the Ministry of Education, Culture, Sports, Science and Technology of Japan. This work was carried out by the joint research program of the Institute for Space-Earth Environmental Research (ISEE), Nagoya University. Yoko Fukuda was supported by Grant-in-Aid for JSPS Fellows 15J07466. Ryuho Kataoka was supported by the Yamada Science Foundation. Ground-based magnetometer data were provided by the Geophysical Institute Magnetometer Array operated by the Geophysical Institute, University of Alaska. More information about this data set is available at <http://magnet.asf.alaska.edu/>. The *Dst* and *AE* indices were provided by WDC for Geomagnetism at Kyoto University. Ground-based high-speed imaging data used in this study, obtained from the sCMOS cameras at Poker Flat Research Range, can be downloaded from the following address: <http://polaris.nipr.ac.jp/~fukuda/cmos/2016/>.

## References

- Beach, R., G. R. Cresswell, T. N. Davis, T. J. Hallinan, and L. R. Sweet (1968), Flickering, a 10-cps fluctuation within bright auroras, *Planet. Space Sci.*, **16**, 1525.
- Berkey, F. T., M. B. Silevitch, and N. R. Parsons (1980), Time sequence analysis of flickering auroras: 1. Application of Fourier analysis, *J. Geophys. Res.*, **85**, 6827–6843, doi:10.1029/JA085iA12p06827.
- Ergun, R. E., et al. (1998), FAST satellite observations of electric field structures in the auroral zone, *Geophys. Res. Lett.*, **25**, 2025–2028, doi:10.1029/98GL00635.
- Erlanson, R. E., and L. J. Zanetti (1998), A statistical study of auroral electromagnetic ion cyclotron waves, *J. Geophys. Res.*, **103**, 4627–4636, doi:10.1029/97JA03169.
- Gurnett, D. A., and L. A. Frank (1972), ELF noise bands associated with auroral electron precipitation, *J. Geophys. Res.*, **77**, 3411–3417, doi:10.1029/JA077i019p03411.
- Gustafsson, G., M. Andre, L. Matson, and H. Koskinen (1990), On waves below the local proton gyrofrequency in auroral acceleration regions, *J. Geophys. Res.*, **95**, 5889–5904, doi:10.1029/JA095iA05p05889.
- Gustavsson, B., J. Lunde, and E. M. Blixt (2008), Optical observations of flickering aurora and its spatiotemporal characteristics, *J. Geophys. Res.*, **113**, A12317, doi:10.1029/2008JA013515.
- Kataoka, R., Y. Fukuda, Y. Miyoshi, H. Miyahara, S. Itoya, Y. Ebihara, D. Hampton, H. Dahlgren, D. Whiter, and N. Ivchenko (2015), Compound auroral micromorphology: Ground-based high-speed imaging, *Earth Planets Space*, **67**, 23, doi:10.1186/s40623-015-0190-6.
- Kunitake, M., and T. Oguti (1984), Spatial-temporal characteristics of flickering spots in flickering auroras, *J. Geomagn. Geoelectr.*, **36**, 121.
- Fukuda, Y., R. Kataoka, Y. Miyoshi, Y. Katoh, T. Nishiyama, K. Shiokawa, Y. Ebihara, D. Hampton, and N. Iwagami (2016), Quasi-periodic rapid motion of pulsating auroras, *Polar Sci.*, **10**, 183–191.
- Lund, E. J., and J. LaBelle (1997), On the generation and propagation of auroral electromagnetic ion cyclotron waves, *J. Geophys. Res.*, **102**, 17,241–17,253, doi:10.1029/97JA01455.
- McFadden, J. P., et al. (1998), Electron modulation and ion cyclotron waves observed by FAST, *Geophys. Res. Lett.*, **25**, 2045–2048, doi:10.1029/98GL00855.
- McHarg, M. G., D. L. Hampton, and H. C. Stenbaek-Nielsen (1998), Fast photometry of flickering in discrete auroral arcs, *Geophys. Res. Lett.*, **25**, 2637–2640, doi:10.1029/98GL01972.
- Michell, R. G., M. G. Mcharg, M. Samara, and D. L. Hampton (2012), Spectral analysis of flickering aurora, *J. Geophys. Res.*, **117**, A03321, doi:10.1029/2011JA016703.

- Omura, Y., J. Pickett, B. Grison, O. Santolik, I. Dandouras, M. Engebretson, P. M. E. Décr  au, and A. Masson (2010), Theory and observation of electromagnetic ion cyclotron triggered emissions in the magnetosphere, *J. Geophys. Res.*, **115**, A07234, doi:10.1029/2010JA015300.
- Paulson, K. V., and G. G. Shepherd (1966), Short-lived brightness oscillations in active auroras, *Can. J. Phys.*, **44**, 921–924.
- Sakanoi, K., and H. Fukunishi (2004), Temporal and spatial structures of flickering aurora derived from high-speed imaging photometer observations at Syowa Station in the Antarctic, *J. Geophys. Res.*, **109**, A01221, doi:10.1029/2003JA010081.
- Sakanoi, K., H. Fukunishi, and Y. Kasahara (2005), A possible generation mechanism of temporal and spatial structures of flickering aurora, *J. Geophys. Res.*, **110**, A03206, doi:10.1029/2004JA010549.
- Semeter, J., M. Zettergren, M. Diaz, and S. Mende (2008), Wave dispersion and the discrete aurora: New constraints derived from high-speed imagery, *J. Geophys. Res.*, **113**, A12208, doi:10.1029/2008JA013122.
- Smith, R. L., and N. Brice (1964), Propagation in multi-component plasmas, *J. Geophys. Res.*, **69**, 5029–5040, doi:10.1029/JZ069i023p05029.
- Stockwell, R. G., L. Mansinha, and R. P. Lowe (1996), Localization of the complex spectrum: The S transform, *IEEE Trans. Signal Process.*, **44**(4), 998–1001, doi:10.1109/78.492555.
- Temerin, M., and R. L. Lysak (1984), Electromagnetic ion cyclotron mode (ELF) waves generated by auroral electron precipitation, *J. Geophys. Res.*, **89**, 2849–2859, doi:10.1029/JA089iA05p02849.
- Temerin, M., J. McFadden, M. Boehm, C. W. Carlson, and W. Lotko (1986), Production of flickering aurora and field-aligned electron flux by electromagnetic ion cyclotron waves, *J. Geophys. Res.*, **91**, 5769–5792, doi:10.1029/JA091iA05p05769.
- Temerin, M., C. Carlson, and J. P. McFadden (1993), The acceleration of electrons by electromagnetic ion cyclotron waves, in *Auroral Plasma Dynamics, Geophys. Monogr. Ser.*, vol. 80, edited by R. L. Lysak, pp. 155–161, AGU, Washington, D. C.
- Whiter, D. K., B. S. Lanchester, B. Gustavsson, N. Ivchenko, and H. Dahlgren (2010), Using multispectral optical observations to identify the acceleration mechanism responsible for flickering aurora, *J. Geophys. Res.*, **115**, A12315, doi:10.1029/2010JA015805.
- Yaegashi, A., T. Sakanoi, R. Kataoka, K. Asamura, Y. Miyoshi, M. Sato, and S. Okano (2011), Spatial-temporal characteristics of flickering aurora as seen by high-speed EMCCD imaging observations, *J. Geophys. Res.*, **116**, A00K04, doi:10.1029/2010JA016333.